Nuclear Engineering and Technology 54 (2022) 764–769

Contents lists available at ScienceDirect

Nuclear Engineering and Technology

journal homepage: www.elsevier.com/locate/net

Technical Note

Static and transient analyses of Advanced Power Reactor 1400 (APR1400) initial core using open-source nodal core simulator KOMODO

Jwaher Alnaqbi [a], Donny Hartanto [b, c, *], Reem Alnuaimi [b], Muhammad Imron [d], Victor Gillette [b, c]

[a] New York University Abu Dhabi, P.O. BOX 129188, Abu Dhabi, United Arab Emirates
[b] Department of Mechanical and Nuclear Engineering, University of Sharjah, P.O. BOX 27272, Sharjah, United Arab Emirates
[c] Nuclear Energy System Simulation and Safety Research Group, Research Institute of Sciences and Engineering, University of Sharjah, P.O. BOX 27272, Sharjah, United Arab Emirates
[d] Department of Nuclear Engineering, Ulsan National Institute of Science and Technology, 50 UNIST-gil, Eonyang-eup, Ulju-gun, Ulsan, 44919, Republic of Korea

ARTICLE INFO

Article history:
Received 29 June 2021
Received in revised form
4 August 2021
Accepted 6 August 2021
Available online 7 August 2021

Keywords:
CASMO-4
KOMODO
Open-source nodal code
Steady-state calculation
Transient simulation
APR-1400

ABSTRACT

The United Arab Emirates is currently building and operating four units of the APR-1400 developed by a South Korean vendor, Korea Electric Power Corporation (KEPCO). This paper attempts to perform APR-1400 reactor core analysis by using the well-known two-step method. The two-step method was applied to the APR-1400 first cycle using the open-source nodal diffusion code, KOMODO. In this study, the group constants were generated using CASMO-4 fuel transport lattice code. The simulation was performed in Hot Zero Power (HZP) at steady-state and transient conditions. Some typical parameters necessary for the Nuclear Design Report (NDR) were evaluated in this paper, such as effective neutron multiplication factor, control rod worth, and critical boron concentration for steady-state analysis. Other parameters such as reactivity insertion, power, and fuel temperature changes during the Reactivity Insertion Accident (RIA) simulation were evaluated as well. The results from KOMODO were verified using PARCS and SIMULATE-3 nodal core simulators. It was found that KOMODO gives an excellent agreement.

1. Introduction

The two-step method has become a standard best practice for reactor core design and analysis, particularly for water-cooled reactors. In this approach, the few-group homogenized cross-sections of each fuel assembly are produced using the neutron transport codes such as CASMO-4 [1] and recently using Monte Carlo codes, for instance, Serpent [2] and OpenMC [3]. First, the cross-sections are typically generated by solving single fuel assembly with reflective boundary conditions using B_1 leakage correction for several burnup points with various fuel temperatures, moderator densities, boron concentrations for pressurized water reactor (PWR), and control rod insertion. Then, the few-group cross-sections are used in a nodal code such as PARCS [4], SIMULATE-3 [5], and KOMODO [6,7] to analyze the reactor behavior at both static and transient conditions. The nodal codes solve the neutron diffusion equation with a short computation time, yet they produce a reasonable level of accuracy compared to the explicit pin-by-pin transport solutions. For example, in recent studies, Serpent and PARCS were utilized effectively in full core modeling of irregular geometry research reactors such as CROCUS [8] and VR-1 [9]. Besides, in verifying new nuclear designs, CASMO-4 and PARCS were used for BWR core design studies [10], while CASMO-4E and SIMULATE-3 were used as calculation tools in evaluating the performance of a new PWR zirconium metal reflector design [11].

Recently, the open-source nodal diffusion code KOMODO (formerly ADPRES) has been developed to solve up to a three-dimensional reactor problem in Cartesian geometry for static and transient conditions with and without thermal-hydraulic feedback. Different multi-group neutron diffusion solvers are available,

* Corresponding author. Department of Mechanical and Nuclear Engineering, University of Sharjah, P.O. BOX 27272, Sharjah, United Arab Emirates.
E-mail address: dhartanto@sharjah.ac.ae (D. Hartanto).

https://doi.org/10.1016/j.net.2021.08.012

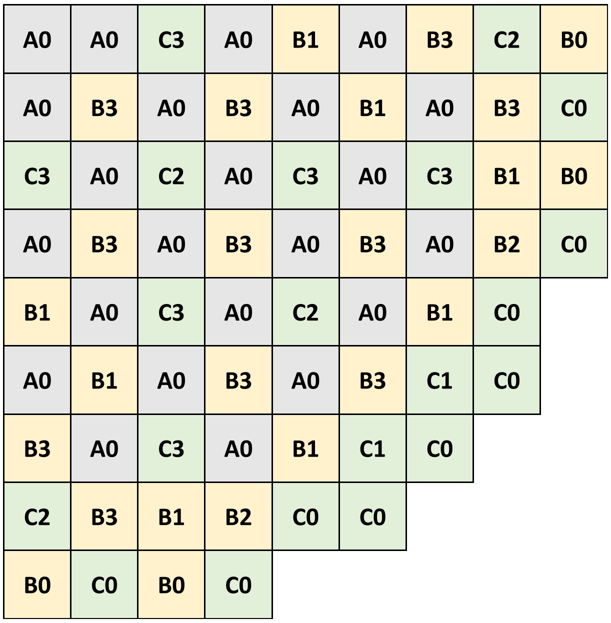

Fig. 1. Initial core fuel loading pattern.

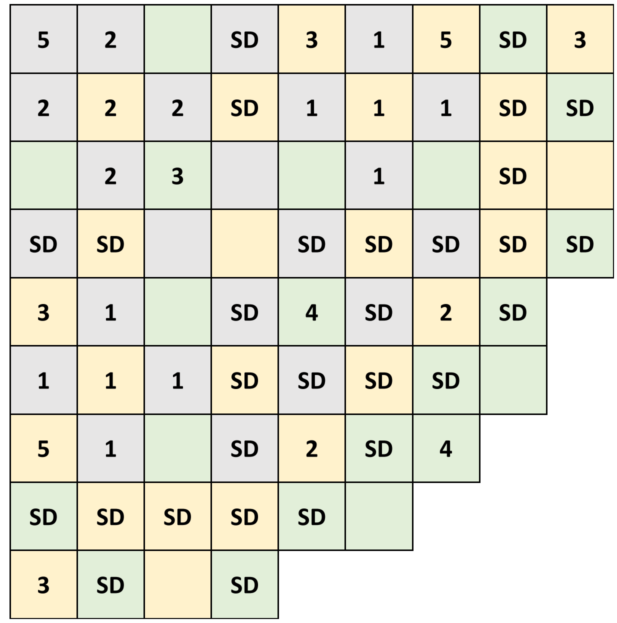

Fig. 2. Simplified control bank configuration.

including Semi-Analytic Nodal Method (SANM), Polynomial Nodal Method (PNM), and the traditional Finite Difference Method (FDM) [7]. Meanwhile, a simplified internal model solving one-dimensional mass and energy conservation equations is adopted to calculate the thermal-hydraulic parameters [7]. The code can perform forward, adjoint, and fixed-source calculations and can be used to find critical boron concentration. As for transient calculations, KOMODO is highly capable of simulating rod ejection accidents. KOMODO has been verified against several reactor benchmark problems, some of them are LMW, NEACRP, and PWR MOX/UO_2 [6,7]. Moreover, it was used recently to evaluate the rod ejection accident in FangJiaShan (FJS) nuclear power plant [12].

In this study, KOMODO was used to simulate the static and transient conditions of the Advanced Power Reactor 1400 (APR1400) being built and operated in the United Arab Emirates (UAE). This work is intended to develop students' reactor analysis capabilities to support the nuclear energy program in the UAE. The APR-1400 reference initial core model was taken from the NURAM-2020-004-00 report [13,14]. The few-group homogenized cross-sections were generated through the fuel lattice code CASMO-4. A utility tool was developed to link CASMO-4 to KOMODO. The static calculations include finding the effective neutron multiplication factor, control rod worth, and critical boron concentration. The solution of the Reactivity Insertion Accident (RIA) simulation from the HZP condition are presented. Finally, the results are verified against PARCS and SIMULATE-3.

Table 2
Comparison of steady-state parameters by KOMODO, PARCS, and SIMULATE-3.

Parameter	KOMODO	PARCS	SIMULATE-3
k_{eff} at ARO	1.148216	1.148326	1.149250
k_{eff} at ARI	0.982255	0.982322	0.982810
CBC at ARO (ppm)	1130.67	1130.52	1129.00
Bank 1 worth (pcm)	1739.23	1738.19	1738.35
Bank 2 worth (pcm)	1070.26	1067.17	1065.30
Bank 3 worth (pcm)	763.85	761.31	763.78
Bank 4 worth (pcm)	242.33	242.87	242.20
Bank 5 worth (pcm)	326.00	325.12	326.03
SD bank worth (pcm)	3286.04	3289.58	3291.60
Total banks worth (pcm)	14714.93	14716.27	14735.80

Table 3
Average error of normalized radial and axial power.

Power	Condition	Reference Codes	PWE	EWE
Radial	ARO	SIMULATE-3	0.459	0.534
		PARCS	0.240	0.312
	ARI	SIMULATE-3	0.444	0.564
		PARCS	0.154	0.344
Axial	ARO	PARCS	1.092	4.345
	ARI		1.125	4.142

Table 1
Fuel assembly type [13,14].

Type	Number of assemblies	Enrichment (wt.%)	Number of rods per assembly	Number of Gd_2O_3 rods per assembly	Gd_2O_3 contents (wt.%)
A0	77	1.71	236	–	–
B0	12	3.14	236	–	–
B1	28	3.14/2.64	172/52	12	8
B2	8	3.14/2.64	124/100	12	8
B3	40	3.14/2.64	168/52	16	8
C0	36	3.64/3.14	184/52	–	–
C1	8	3.64/3.14	172/52	12	8
C2	12	3.64/3.14	168/52	16	8
C3	20	3.64/3.14	120/100	16	8

1.573 -0.38 -0.70	1.426 -0.40 -0.84	1.502 -0.39 0.20	1.269 -0.27 -0.71	1.425 -0.22 0.35	1.137 -0.11 -0.44	1.000 0.04 0.70	0.870 0.20 0.69	0.743 0.43 0.13
1.426 -0.41 -0.84	1.457 -0.40 0.14	1.295 -0.28 -0.77	1.335 -0.30 0.30	1.209 -0.23 -0.66	1.287 -0.10 0.47	0.948 0.05 -0.32	0.822 0.27 0.61	0.765 0.54 0.39
1.502 -0.40 0.20	1.295 -0.28 -0.77	1.454 -0.32 0.28	1.194 -0.19 -0.67	1.296 -0.22 0.39	1.052 -0.01 -0.48	1.029 0.05 0.58	0.838 0.26 0.48	0.677 0.47 0.15
1.269 -0.28 -0.71	1.335 -0.31 0.30	1.194 -0.19 -0.67	1.212 -0.19 0.41	1.058 -0.13 -0.57	1.043 -0.01 0.48	0.875 0.17 -0.46	0.769 0.40 0.39	0.520 0.58 0.00
1.425 -0.23 0.35	1.209 -0.24 -0.66	1.296 -0.22 0.39	1.058 -0.13 -0.57	1.140 -0.07 0.53	0.898 0.10 -0.56	0.915 0.19 0.22	0.795 0.42 -0.13	
1.137 -0.13 -0.44	1.287 -0.11 0.47	1.052 -0.02 -0.48	1.043 -0.01 0.48	0.898 0.09 -0.56	0.827 0.19 0.36	0.771 0.39 0.26	0.532 0.45 -0.38	
1.000 0.02 0.70	0.948 0.03 -0.32	1.029 0.04 0.58	0.875 0.16 -0.46	0.915 0.19 0.22	0.771 0.39 0.26	0.550 0.47 -0.36		
0.870 0.17 0.69	0.822 0.24 0.61	0.838 0.25 0.48	0.769 0.39 0.39	0.795 0.42 -0.13	0.532 0.45 -0.38			
0.743 0.42 0.69	0.765 0.51 0.61	0.677 0.46 0.48	0.520 0.56 0.39				Radial Power KOMODO Rel. Diff. w/ PARCS (%) Rel. Diff. w/ SIMULATE-3 (%)	

Fig. 3. Normalized radial power distribution at ARO.

This paper is organized as follows: Section 2 discusses the APR1400 initial core model and calculation methodology. Section 3 presents the steady-state results, and the transient results are discussed in Section 4. Finally, the conclusions and recommendations for future works are given in Section 5.

2. Calculation model and methodology

2.1. APR-1400 initial core

The Advanced Power Reactor APR-1400 is a Generation-III+ pressurized light water reactor with two reactor coolant loops, developed by Korea Electric Power Corporation (KEPCO) by integrating the technology and features of OPR1000 to enhance plant safety and efficiency. Four units of the APR-1400 reactor with a design life of 60 years are being jointly constructed and operated by KEPCO and Emirates Nuclear Energy Corporation (ENEC) in the Barakah site to supply up to 25% of the United Arab Emirates' electricity grid. The first unit has successfully entered the commercial operation phase.

Radially, the APR-1400 reactor core contains 241 PLUS7 advanced fuel assemblies developed by Korea Nuclear Fuel (KNF) arranged into 17x17 configuration, producing 3983 MWth at full power with a net efficiency of 35.1%. While axially, the core has an active length of 3.81 m. Each fuel assembly contains 236 fuel rods positioned in a 16 $\times$ 16 array with four guide thimbles and one central instrumentation tube fused with the grid. The fuel pellets, made of uranium dioxide (UO_2), are encapsulated in the advanced ZIRLO fuel cladding. The detailed geometry of the fuel rod and assembly is available in Barr et al. [14].

A quarter initial core loading pattern is illustrated in Fig. 1, and the fuel assembly types of the initial core are summarized in Table 1. Nine fuel assembly types are used in the initial core, with low enrichments between 1.71 wt% and 3.64 wt%, where six of them are embedded with 12 or 16 fuel pins mixed with 8 wt% of Gd_2O_3 burnable poison per assembly. An axial cutback of about 15.24 cm is located at each top and bottom of B and C fuel assemblies. In the cutback region, the uranium enrichment is uniform with about 2 wt%. The fuel is mainly consumed through three cycles, each last for 18 months with a maximum of 60,000 MWD/MTU fuel rod burnup.

The APR-1400 is regulated by 93 control element assemblies (CEAs), composed of 12-fingered and 4-fingered configurations. These CEAs are grouped into seven banks, in which five banks (banks 1, 2, 3, 4, and 5) are used for power maneuvering, and the other two banks (A and B) are for immediate reactor shutdown. To simplify the modeling, the 12-fingered configuration is modified to a 4-fingered configuration so that when the control rods are inserted, they occupy all guide tubes. The simplification results in additional 16 control rods insertion. Moreover, the two shutdown banks (SD) were merged into one. This modification is demonstrated in Fig. 2. The detailed geometry of the control rods is available in Barr et al. [14]. The control rod uses B_4C as the absorber material.

2.2. Methodology

The lattice transport code CASMO-4 generated the few-group

0.879 -0.11 -0.34	0.993 -0.15 -0.40	1.866 -0.17 0.43	1.198 -0.07 -0.42	1.157 -0.13 0.26	0.690 -0.03 -0.43	0.508 0.06 0.39	0.392 0.38 0.26	0.308 0.71 -0.65
0.993 -0.16 -0.40	1.190 -0.12 0.50	1.379 0.08 -0.44	1.752 0.10 0.57	1.284 0.10 -0.39	0.988 -0.05 0.30	0.545 0.15 -0.37	0.427 0.23 0.00	0.391 0.59 -0.51
1.866 -0.18 0.43	1.379 -0.09 -0.44	2.467 0.14 0.65	3.264 0.09 -0.34	2.761 0.13 0.58	1.025 -0.07 -0.39	0.954 0.00 0.31	0.539 0.32 0.00	0.573 0.61 -0.70
1.198 -0.08 -0.42	1.752 -0.10 0.57	3.264 0.09 -0.34	3.502 0.11 0.66	1.585 -0.10 -0.32	0.928 -0.06 0.43	0.533 0.17 -0.56	0.430 0.40 -0.23	0.312 0.74 -0.64
1.157 -0.15 0.26	1.284 -0.11 -0.39	2.761 0.13 0.58	1.585 -0.11 -0.32	1.163 -0.14 0.52	0.570 0.07 -0.53	0.481 0.27 -0.21	0.413 0.39 -0.97	
0.690 -0.04 -0.43	0.988 -0.06 0.3	1.025 -0.08 -0.39	0.928 -0.08 0.43	0.570 0.05 -0.53	0.440 0.09 0.00	0.401 0.35 -0.5	0.407 0.66 -0.98	
0.508 0.04 0.39	0.545 0.13 -0.37	0.954 -0.01 0.31	0.533 0.17 -0.56	0.481 0.25 -0.21	0.401 0.35 -0.50	0.271 0.44 -1.48		
0.392 0.36 0.26	0.427 0.23 0.00	0.539 0.32 0.00	0.430 0.40 -0.23	0.413 0.36 -0.97	0.407 0.66 -0.98			
0.308 0.68 -0.65	0.391 0.56 -0.51	0.573 0.59 -0.70	0.312 0.74 -0.64					

Radial Power KOMODO
Rel. Diff. w/ PARCS (%)
Rel. Diff. w/ SIMULATE-3 (%)

Fig. 4. Normalized radial power distribution at ARI.

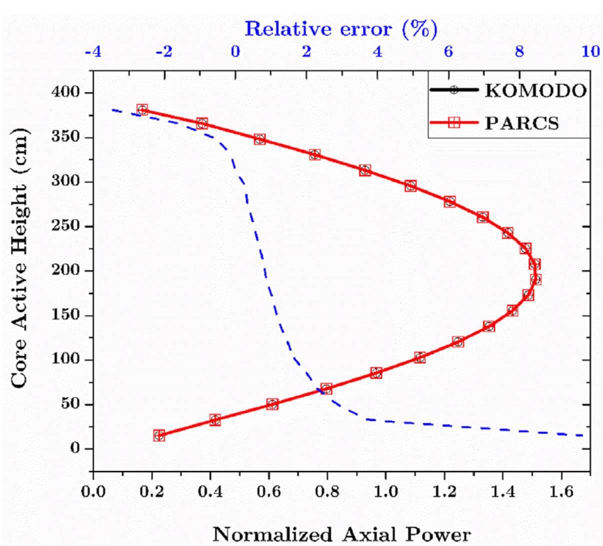

Fig. 5. Normalized axial power distribution at ARI.

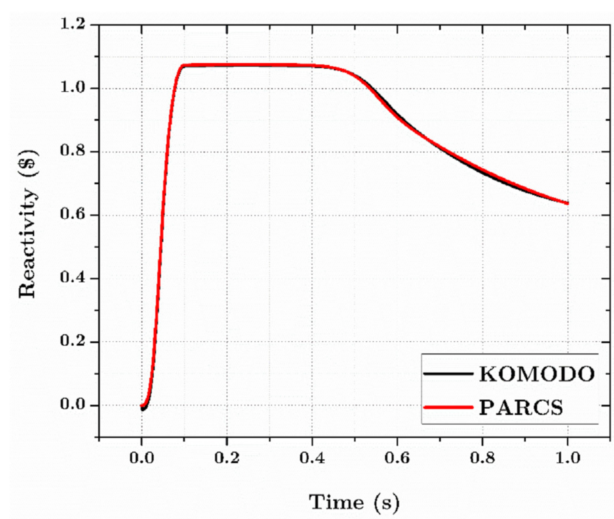

Fig. 6. Transient reactivity.

homogenized cross-sections of the fuel and non-fuel regions. CASMO-4 is a two-dimensional multi-group method of characteristics transport lattice code developed by Studsvik Scandpower. It is widely used to perform lattice burnup calculations and generate few-group homogenized cross-sections for light water reactors (LWRs). In CASMO-4, 70 energy-group microscopic cross-sections derived from the ENDF/B-VI library were used, then condensed into two energy groups with cut-off energy at 0.625 eV. In this work, the automatic branching option in CASMO-4 was utilized to generate the few-group homogenized cross-sections. The reference condition was set at a fuel temperature of 900 K, moderator temperature of 580.4 K, and boron concentration of 600 ppm. Meanwhile, a model consisting of a fuel lattice next to a 50 cm thick

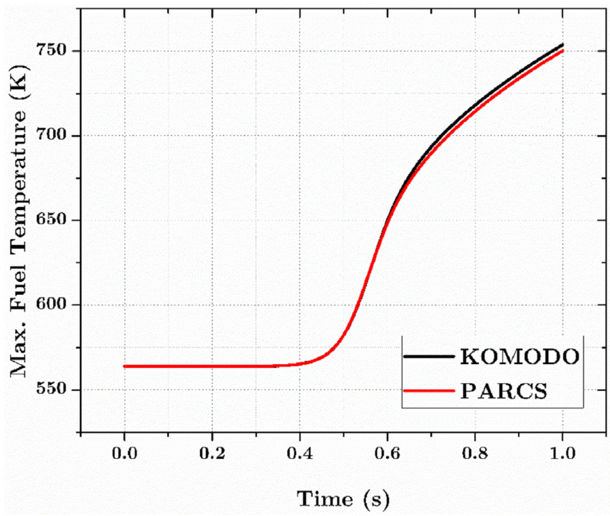

Fig. 7. Transient fuel temperature.

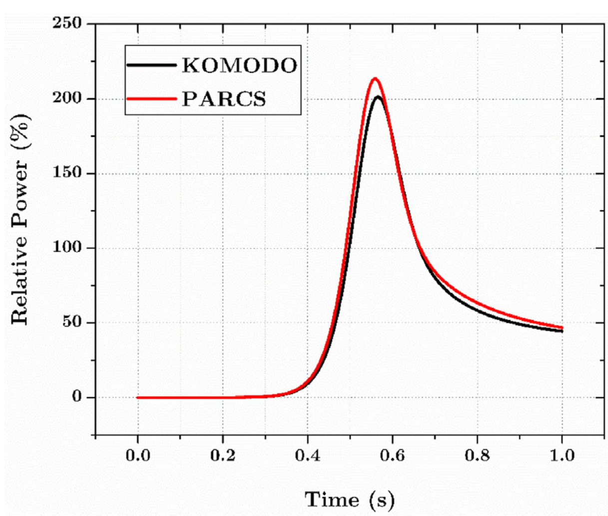

Fig. 8. Transient relative power.

Table 4
Transient solutions.

Codes	Peak Time (s)	Peak Power (%)	Peak Reactivity (%)	Integral Power (%-second)
KOMODO	0.246	201.45	1.0730	50.36
PARCS	0.238	213.55	1.0753	53.76

water reflector generates the few-group homogenized cross-sections for radial and axial reflectors.

The generated few-group cross-sections are then inserted in the three nodal codes: KOMODO, PARCS, and SIMULATE-3. In KOMODO, the semi-analytic nodal method [15] was used to solve both static and transient scenarios. A quarter core model is adopted in the nodal core simulation. The APR-1400 initial core is divided to 19x19 nodes in the radial direction and 24 nodes in the axial direction. The active core is divided to 22 axial nodes, and one axial node with a thickness of 50 cm is located at the top and the bottom of the core. The assembly discontinuity factors (ADFs) were considered in the calculation.

3. Steady-state simulations

The steady-state calculations were performed at hot zero power (HZP) condition, defined by having a reactor power of 1E-5%. The evaluated parameters include the effective neutron multiplication factor k_{eff}, control rod worth, and critical boron concentration, as summarized in Table 3. The static calculations were carried out for both all rods out (ARO) and all rods in (ARI) conditions. The absolute relative difference of the multiplication factor at ARO between KOMODO and PARCS is relatively small, about 11 pcm. In contrast, the difference is slightly higher with SIMULATE-3, which is just over 100 pcm. However, these differences are slightly lower at ARI, about 7 pcm and 56 pcm against PARCS and SIMULATE-3, respectively. Interestingly, the differences in the effective multiplication factors do not affect much on the critical boron concentration (CBC). The difference in the CBC between SIMULATE-3 and other nodal codes is less than 1 ppm.

In the static calculations, the CR worth of each bank was obtained as this information is crucial for reactor power maneuvering and nuclear safety. The bank worth was calculated such that the chosen bank is inserted while others are withdrawn. As shown in Table 2, the results among the three codes are similar, with maximum deviations of about 4 pcm and 6 pcm against PARCS and SIMULATE-3, respectively. As expected, the SD bank has the highest worth, while bank 4 has the lowest as it is inserted into 8 fuel assemblies only, in addition to its position near the periphery of the core. It is also noticed that when all banks are inserted, the core is at a subcritical state.

Figs. 3 and 4 show KOMODO's relative power distribution along with the relative differences with PARCS and SIMULATE-3 at the ARO and ARI conditions, respectively. The maximum relative difference between KOMODO and PARCS is 0.58% and 0.74% at ARO and ARI conditions, respectively. Meanwhile, it is −0.84% and 1.48% with SIMULATE-3 at ARO and ARI conditions, respectively. The three codes show an excellent agreement of results. At the ARI condition, the maximum difference among the three codes is located at the periphery of the core, next to the radial reflector region, as shown in Fig. 4.

Fig. 5 displays the reactor axial power profiles of KOMODO and PARCS at ARI condition where the difference in the trends is insignificant. Starting from the undermost reflector, followed by the bottom cutback region, the axial power increases until it peaks at about 1.5 in the middle of the active fuel region of the assembly. After surpassing the active fuel mid-region, the power decreases until it reaches zero as it approaches the top reflector. A similar trend is observed in the ARO condition. The maximum relative error of the axial power between KOMODO and PARCS is located adjacent to the axial reflector, where the axial power is relatively small.

The average error of the normalized radial and axial power distribution was found using the power-weighted error (PWE) and error-weighted error (EWE) where they are given by the equations [16] below. As summarized in Table 3, KOMODO has an excellent agreement with the other codes by having PWE and EWE values less than 1.125% and 4.345%, respectively.

$$PWE = \frac{\sum_i |e_i| ref_i}{\sum_i ref_i} \tag{1}$$

$$EWE = \frac{\sum_i |e_i||e_i|}{\sum_i |e_i|} \tag{2}$$

where:

$$e_i = \frac{KOMODO_i - ref_i}{ref_i} \times 100 \quad (3)$$

4. Transient simulations

The Reactivity Insertion Accident (RIA) simulation from the HZP condition was conducted to examine the reactivity and power changes due to the control rod ejection. The challenge of simulating an RIA at HZP condition lies in the exponential power increase since the negative Doppler reactivity feedback takes longer to effect. However, by virtue of the inherent safety characteristic of typical LWRs, the reactivity feedback from fuel and moderator would eventually suppress the power increase.

In the RIA simulation, KOMODO results were compared against PARCS' solutions. All banks except the SD were inserted at the beginning of this transient, and boron was added to the core to put it into a critical state. The critical boron concentration was found to be about 747.21 and 747.77 ppm for KOMODO and PARCS, respectively. Within 0.1 s, both banks 4 and 5 were ejected from the core. The transient accident duration time was set to 1 s.

Comparisons of the transient core reactivity, fuel temperature, and relative power are presented in Figs. 6–8, respectively. The quantitative results of the two codes are summarized in Table 4, showing a noticeable excellent agreement. Fig. 6 shows that immediately after ejecting banks 4 and 5, the core reactivity sharply increased due to absorption reduction then started to saturate when the banks were fully withdrawn. Afterward, it decreased as the fuel temperature was increasing after about 0.4 s. This phenomenon is a result of the fuel Doppler temperature reactivity feedback and negative reactivity feedback from both moderator temperature and density. The maximum power in this scenario is about 201.45% by KOMODO, while it is 213.55% by PARCS. Overall, it is shown that both KOMODO and PARCS results concur very well.

5. Conclusions

In this work, steady and transient analyses have been conducted for the APR-1400, the reactor type being built and operated in the United Arab Emirates. The fuel lattice transport code CASMO-4 was used to generate the group constants which were subsequently supplied to the open-source nodal code KOMODO. The results were then compared to the other nodal codes PARCS and SIMULATE-3. It was found that KOMODO results have a good agreement with PARCS, but some deviations in the effective multiplication factors were observed against SIMULATE-3. As for the transient results, the solutions were compared only against PARCS, and both of the nodal codes provided almost similar results. For future works, the Monte Carlo code will be applied to generate the few-group homogenized cross-sections of the APR1400, and KOMODO results at both steady-state and transient calculations will be compared against the Monte Carlo method solutions.

Declaration of competing interest

The authors declare that they have no known competing financial interests or personal relationships that could have appeared to influence the work reported in this paper.

Acknowledgment

This research was supported by the Office of Vice Chancellor for Research & Graduate Studies, University of Sharjah, under grant no. 210204081171.

References

[1] Studsvik Scandpower Inc, CASMO-4 A Fuel Assembly Burnup Program User's Manual, Studsvik Scandpower Inc., 2009. SSP-09/443 - U Rev 0.
[2] J. Leppänen, et al., The serpent Monte Carlo code: status, development and applications in 2013, Ann. Nucl. Energy 82 (2015) 142–150.
[3] P.K. Romana, et al., OpenMC: a state-of-the-art Monte Carlo code for research and development, Ann. Nucl. Energy 82 (2015) 90–97.
[4] T. Downar, et al., PARCS: Purdue advanced reactor core simulator, in: Proceedings of PHYSOR 2002, Seoul, Korea, 2002, pp. 7–10. October.
[5] Studsvik Scandpower Inc, SIMULATE-3 Advanced Three-Dimensional Two-Group Reactor Analysis Code, Studsvik Scandpower Inc., 2009. SSP-09/447 - U Rev 0.
[6] M. Imron, Development and verification of open reactor simulator ADPRES, Ann. Nucl. Energy 133 (2019) 580–588.
[7] M. Imron, D. Hartanto, PWR MOX/UO_2 transient benchmark calculation using Monte Carlo serpent 2 code and open nodal core simulator ADPRES, ASME J of Nuclear Rad Sci 7 (3) (2020), 031603.
[8] D.J. Siefman, et al., Full core modeling techniques for research reactors with irregular geometries using serpent and PARCS applied to the CROCUS reactor, Ann. Nucl. Energy 85 (2015) 434–443.
[9] F. Fejt, J. Frybort, Analysis of a small-scale reactor core with PARCS/serpent, Ann. Nucl. Energy 117 (2018) 25–31.
[10] F.Y. Odeh, W.S. Yang, Core design optimization and analysis of the Purdue novel modular reactor (NMR-50), Ann. Nucl. Energy 94 (2016) 288–299.
[11] J. Choe, et al., Performance evaluation of Zircaloy reflector for pressurized water reactors, Int. J. Energy Res. 40 (2) (2016) 160–167.
[12] Li Z., et al., Development and verification of PWR core transient coupling calculation software, Nuclear Eng. Technol. In press.
[13] K. Barr, S. Choi, B. Kochunas, Verification of MPACT for the APR1400 Benchmark, Nuclear Reactor Analysis & Methods Group, University of Michigan, 2020. NURAM-2020-004-00.
[14] S. Yuk, et al., APR-1400 Reactor Core Benchmark Problems, 2019. KAERI/TR-7822/2019.
[15] V.G. Zimin, H. Ninokata, Nodal neutron Kinetics model based on nonlinear iteration Procedure for LWR analysis, Ann. Nucl. Energy 25 (8) (1998) 507–528.
[16] T. Kozlowski, T.J. Downar, PWR MOX/UO_2 Core Transient Benchmark vol. 20, Nuclear Energy Agency, OECD, NEA/NSC/DOC, 2006.